

Coherent control of birefringence and optical activity

Seyedmohammad A. Mousavi, ¹ Eric Plum, ^{1,a)} Jinhui Shi, ^{1,2} and Nikolay I. Zheludev^{1,3,b)} ¹Optoelectronics Research Centre and Centre for Photonic Metamaterials, University of Southampton, Southampton SO17 1BJ, United Kingdom

²Key Laboratory of In-Fiber Integrated Optics of Ministry of Education, College of Science, Harbin Engineering University, Harbin 150001, China

³Centre for Disruptive Photonic Technologies, Nanyang Technological University, Singapore 637378, Singapore

(Received 30 May 2014; accepted 1 July 2014; published online 9 July 2014)

We show that polarization effects due to anisotropy and chirality affecting a wave propagating through a thin slab of material can be controlled by another electromagnetic wave. No nonlinearity of the metamaterial slab is required and the control can be exercised at arbitrarily low intensities. In proof-of-principle experiments with anisotropic and chiral microwave metamaterials, we show that manifestations of linear and circular birefringence and dichroism can be modulated by the control wave from their maximum value to zero. © 2014 AIP Publishing LLC. [http://dx.doi.org/10.1063/1.4890009]

Anisotropic materials can show linear birefringence and dichroism, while materials composed of chiral molecules that cannot be superimposed with their mirror image can show circular birefringence and dichroism (optical activity). Polarization phenomena associated with anisotropy and chirality are normally observed in a traveling wave. However, as illustrated by Fig. 1, if a thin slab of material is placed at an electric anti-node of a standing wave it will experience twice the electric field compared to the traveling wave illumination, while no electric excitation occurs if the slab is placed at an electric-field node. Similarly, the slab placed at the magnetic-field anti-node or node will experience enhanced or zero magnetic excitation, respectively. In fact, the conditions of a standing wave formed by two counter-propagating waves can be relaxed. The waves can propagate at an arbitrary angle as long as the slab is placed in their intersection point with the plane of the slab forming equal angles with the wave front normals as shown. In this case, at each point of the thin slab the phase difference between the waves will be the same and the above consideration holds. Coherent optical effects are now attracting considerable attention^{1–11} and coherent control of absorption¹² and coherent spectroscopic techniques¹³ have been demonstrated recently in metamaterials. Here, we explore how coherent interaction of two waves on a thin sheet of material can be used to control the polarization effects associated with linear birefringence and optical activity of the slab.

We studied the control of manifestations of optical anisotropy and optical activity in metamaterial samples in the microwave part of the spectrum between 3 and 12 GHz (100–25 mm wavelength) using a microwave anechoic chamber, broadband microwave antennas, and a vector network analyzer. Both control and signal antennas were equipped with collimating lenses and were fed with the same signal through identical cables, while the relative phase delay was altered by moving the control wave antenna along the beam direction. We compared the experimentally measured data with full 3D

Maxwell simulations. Experiments were conducted with a small angle of incidence (13°) to allow the control and receiving antennas to be placed next to each other, while simulations correspond to normal incidence conditions.

Control of optical manifestations of anisotropy has been demonstrated in a metamaterial array consisting of asymmetrically split wire rings, Figs. 2(a) and 2(b). The sample had an overall diameter of 220 mm and a thickness of 1.6 mm. It consisted of a square array of $15 \times 15 \text{ mm}^2$ meta-molecules. At normal incidence, the structure supports ordinary and extraordinary eigenpolarizations oriented parallel and perpendicular to the pattern's line of symmetry. Here, the polarization effects associated with optical anisotropy can be easily seen for illumination with incident linear polarization intermediate between the eigenpolarizations, for instance, at 45° to its line of mirror symmetry, as in our experiments. As illustrated by Figs. 2(c) and 2(d), under these illumination conditions, the anisotropic metamaterial dramatically changes the azimuth and ellipticity angle of the transmitted beam across almost the entire investigated spectral range. In particular, it behaves like a quarter wave plate around 9 GHz, where the transmitted beam converts into left-handed circular polarization.

If the anisotropic metamaterial is also exposed to the control wave of the same polarization as the wave probing

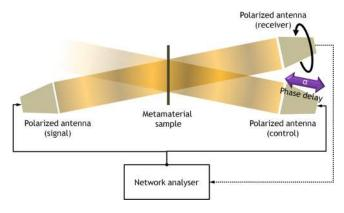


FIG. 1. Sketch of arrangements for experiments on coherent control of optical manifestations of anisotropy and chirality.

a)Electronic mail: erp@orc.soton.ac.uk

b) Electronic mail: niz@orc.soton.ac.uk. URL: www.nanophotonics.org.uk.

FIG. 2. Coherent control of optical manifestations of anisotropy. Anisotropic unit cell (a) and fragment (b) of the metamaterial array consisting of asymmetrically split wire rings. The incident polarization E is indicated by a double arrow. Single beam polarization azimuth rotation (c) and ellipticity angle (d) of the transmitted signal beam. Coherently controlled polarization azimuth rotation (e) and ellipticity (f) as a function of the phase difference α between the additional control and the signal incident beams, which have parallel polarizations. (g) and (h) The same optical properties for a selected frequency of 9.1 GHz, where the metamaterial behaves as a coherently controlled polarization rotator.

anisotropy, see Figs. 2(e)–2(h), the polarization of the detected signal output wave strongly depends on the phase difference α between the control and signal input beams. For in-phase excitation $(\alpha=0^\circ)$, the electric field at the metamaterial slab doubles leading to an increase in the structure's scattered fields and changes in the observed polarization effects. For anti-phase excitation $(\alpha=180^\circ)$, destructive interference of the incident electric fields prevents excitation of the metamaterial structure, thus, suppressing polarization effects in the detected beam.

As a result, the metamaterial acts as a polarization rotator controlled by the phase difference α in the entire spectral range of measurements from 6.5 GHz to 11.5 GHz. At 9.1 GHz, where the ellipticity of the output polarization remains small, it performs as a nearly perfect controllable polarization rotator. Similarly, a profound ellipticity modulation can be achieved between 6 and 7 GHz, which allows the output beam to be continuously tuned from right-handed circular polarization to left-handed almost circular polarization.

Control of optical activity due to chirality was demonstrated in a metamaterial consisting of a square array of $15 \times 15 \text{ mm}^2$ metamolecules containing mutually twisted rosette metal patterns in parallel planes spaced by a dielectric substrate of 1.6 mm thickness, Figs. 3(a) and 3(b).

Close to normal incidence, the metamaterial's optical properties are polarization azimuth independent. As shown by Figs. 3(c) and 3(d), for single wave measurements, the metamaterial exhibits large circular birefringence and circular dichroism near its resonances at about 4.9 and 6.1 GHz.

The metamaterial's polarization response is affected by the control wave of the same polarization as the signal beam, see Figs. 3(e)-3(h). Similarly to the case of anisotropy, the polarization state of the transmitted signal wave strongly depends on the phase difference between the signal and control waves and can be modulated in a large range. However, in contrast to the case of the anisotropic metamaterial there is no special phase α where all polarization effects vanish suggesting that magnetic excitation of the metamaterial plays an important role. Indeed, the 4.9 GHz resonance has previously been identified as a magnetic resonance leading to a negative effective permeability and negative refractive index. 14,15 The associated magnetic excitation mode is characterized by counter propagating currents in the metal patterns on opposite sides of the substrate (inset to Fig. 3(d)). Such a magnetic resonance can be excited effectively at the magnetic anti-node. At the 4.9 GHz resonance, the metamaterial also acts as a coherent polarization rotator that

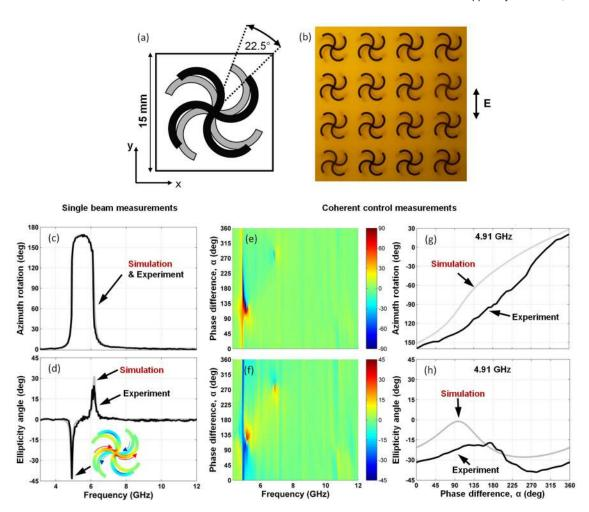


FIG. 3. Coherent control of optical manifestations of chirality. 3D-chiral unit cell (a) and fragment (b) of a metamaterial array consisting of mutually twisted wire patterns in parallel planes. The incident polarization E is indicated by a double arrow. Single beam polarization azimuth rotation (c) and ellipticity angle (d) of the transmitted signal beam. The inset shows the x-component of the current density at the 4.9 GHz resonance. Coherently controlled polarization azimuth rotation (e) and ellipticity (f) as a function of the phase difference α between the additional control and the signal incident beams, which have parallel polarizations. (g) and (h) The same optical properties for a selected frequency of 4.91 GHz, where the metamaterial behaves as a coherently controlled polarization rotator.

uniquely maps the phase α onto the polarization azimuth of the elliptically polarized output beam, see Figs. 3(g) and 3(h). We note that simulations and experiments show the same qualitative behavior. The quantitative differences in the latter figure may be due to the slightly different angles of incidence in coherent control simulations (0°) and coherent control experiments (13°), resulting from having to place the control and receiving antennas side by side.

While the experimental results reported here were measured in the microwave part of the spectrum, the same approach to coherent control of polarization effects can be easily applied across the electromagnetic spectrum. Moreover, coherent polarization control has tremendous potential for ultrafast modulation of electromagnetic waves. For non-resonant conditions, the modulation bandwidth should approach the frequency of the electromagnetic wave itself, while achievable modulation rates for resonant polarization control should be lower by about the resonance quality factor. Applied to the optical telecommunications band around 1.5 μ m, where metamaterial resonances typically have quality factors on the order of 10, this promises modulation rates on the order of 10 THz for resonant

In summary, we show that coherent control of polarization effects in a thin slab of material can be achieved by excitation of the material slab with a control wave that is coherent with the wave probing the polarization effect.

The authors are grateful to Xu Fang, Kevin MacDonald, and Ming Lun Tseng for fruitful discussions. This work was supported by the MOE Singapore (Grant MOE2011-T3-1-005), the Leverhulme Trust, the Royal Society and the UK's Engineering and Physical Sciences Research Council through the Nanostructured Photonic Metamaterials Programme Grant. J.S. acknowledges support from the National Science Foundation of China (Grant No. 61201083).

¹M. I. Stockman, S. V. Faleev, and D. J. Bergman, Phys. Rev. Lett. 88, 067402 (2002).

²X. Li and M. I. Stockman, Phys. Rev. B 77, 195109 (2008).

³S. B. Choi, D. J. Park, Y. K. Jeong, Y. C. Yun, M. S. Jeong, C. C. Byeon, J. H. Kang, Q.-H. Park, and D. S. Kim, Appl. Phys. Lett. 94, 063115

⁴T. Utikal, M. I. Stockman, A. P. Heberle, M. Lippitz, and H. Giessen, Phys. Rev. Lett. 104, 113903 (2010).

⁵T. S. Kao, S. D. Jenkins, J. Ruostekoski, and N. I. Zheludev, Phys. Rev. Lett. 106, 085501 (2011).

- ⁶B. Gjonaj, J. Aulbach, P. Johnson, A. Mosk, L. Kuipers, and A. Lagendijk, Nat. Photonics 5, 360 (2011).
- ⁷W. Wan, Y. Chong, L. Ge, H. Noh, A. D. Stone, and H. Cao, Science 331, 889 (2011).
- ⁸Z. Li, S. Zhang, N. J. Halas, P. Nordlander, and H. Xu, Small 7, 593 (2011).
- ⁹M. Miyata and J. Takahara, Opt. Express **20**, 9493 (2012).
- ¹⁰J. W. Yoon, G. M. Koh, S. H. Song, and R. Magnusson, Phys. Rev. Lett. 109, 257402 (2012).
- ¹¹D. Brinks, M. Castro-Lopez, R. Hildner, and N. F. van Hulst, Proc. Natl.
- Acad. Sci. U.S.A. **110**, 18386 (2013).
 ¹²J. Zhang, K. F. MacDonald, and N. I. Zheludev, Light: Sci. Appl. **1**, e18
- ¹³X. Fang, M. L. Tseng, D. P. Tsai, and N. I. Zheludev, e-print arXiv:1312.0524.
- ¹⁴A. V. Rogacheva, V. A. Fedotov, A. S. Schwanecke, and N. I. Zheludev, Phys. Rev. Lett. 97, 177401 (2006).
- ¹⁵E. Plum, J. Zhou, J. Dong, V. A. Fedotov, T. Koschny, C. M. Soukoulis, and N. I. Zheludev, Phys. Rev. B 79, 035407 (2009).